phys. stat. sol. (c) **4**, No. 10, 3924–3927 (2007) / **DOI** 10.1002/pssc.200675815

Reflection high-energy positron diffraction study of surface super-structures

A. Kawasuso[*], **Y. Fukaya, K. Hayashi, M. Hashimoto,** and **A. Ichimiya**

Advanced Science Research Center, Japan Atomic Energy Agency, 1233, Watanuki, Takasaki, Gunma 370-1292, Japan

Received 23 July 2006, accepted 1 August 2007
Published online 13 August 2007

PACS 41.75.Fr, 61.18.–j, 61.30.Hn, 68.47.Fg

In this work, we studied a few surface super-structures using reflection high-energy positron diffraction (RHEPD). We found that the RHEPD pattern from the Si(111)-7×7 surface exhibits different features from that of electron diffraction. The difference is explained as a strong thermal diffuse scattering of positrons at the first surface layer. We also studied the phase transition of the Si(111)-√3×√3-Ag surface. We found that the surface sensitive diffraction spots exhibit peculiar temperature dependences. Based on theoretical considerations, we interpreted the temperature dependences in terms of the order-disorder phase transition. Furthermore, we succeeded in determining a unique structure of the Si(111)-√21×√21-Ag surface.

1 Introduction One important aspect in the interactions between high-energy positrons and matter is the negligibly small correlation effect. Therefore, the diffraction processes of high-energy positrons are described mainly using the Hartree-Fock (crystal) potential. Strictly to say, the scattering cross sections and hence atomic form factors for positrons and electrons are different due to the different phase shifts of the scattered waves. In high-energy region, however, the lowest-order Born approximation is adequate. Therefore, the crystal potential for positrons may be close to the absolute value of that for electrons. The crystal potential for positrons is thus positive. Consequently, a positron beam is totally reflected at the first surface layer when small enough incident angles. The total reflection never occurs in the case of electrons. The reflection high-energy positron diffraction (RHEPD) is suited to study the surface properties without any disturbances from the bulk [1].

Using the electro-magnetic lenses we developed a positron beam, which is more coherent as compared to the previous beam [2]. This leads to the successful observation of the fractional order diffraction spots. In this article, we report the difference in positron and electron diffraction patterns. As the applications of RHEPD, we also report the observation of the phase transition of the Si(111)-√3×√3-Ag which is still under the debate [3–7] and the determination of the structure of the Si(111)-√21×√21-Ag [8–11].

2 Experiment Samples were prepared from a mirror-polished Si(111) substrate. After cleaning using ethanol and ultra-pure water, the samples were transferred into the ultra-high vacuum chamber evacuated to a base pressure of 1×10^{-8} Pa. To form the Si(111)-7×7 surface, the sample flashing was carried out at 1200 °C by direct resistive heating. The Si(111)-√3×√3-Ag surface was obtained by depositing 1ML of Ag atoms onto the Si(111)-7×7 surface at 550 °C. Furthermore, the Si(111)-√21×√21-Ag surface was obtained by depositing 0.14 ML of Ag atoms onto the Si(111)-√3×√3-Ag surface at 150 K. A well-focused (1 mm diameter) positron beam with an energy of 10 keV, a flux of 10^4 e^+/sec and a brightness

[*] Corresponding author: e-mail: kawasuso.atsuo@jaea.go.jp

of 10^7 e^+/sec/cm^2/rad^2/V was generated using a ^{22}Na source (3.7GBq), a tungsten-mesh moderator, an improved positron gun and electro-magnetic lenses. The details were described elsewhere [2]. The beam was irradiated onto the sample surfaces at glancing angles of 0.3-6.5° and back-reflected beam was detected using a multi-channel plate with a phosphor plane (Hamamatsu F2226-24P). The phosphor plane images were observed using a charge-coupled device camera connected to a personal computer.

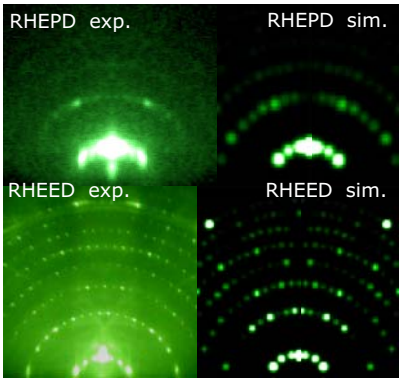

Fig. 1 RHEPD and RHEED patterns from the Si(111)-7×7 surface obtained in experiments and simulations.

3 Results and discussion

3.1 RHEPD pattern of Si(111)-7×7 surface Figure 1 shows the comparison between the RHEPD and RHEED patterns from the Si(111)-7×7 surface. The glancing angle is 1.95° that satisfies the total reflection condition for positrons. In the RHEPD pattern, the fractional order spots can be specified but image itself is somewhat blurry as compared to the RHEED one. This is not due to the beam quality and attributed to the different sensitivity of positrons and electrons to the surface. Most positrons are reflected at the first and second surface layers where the vibration amplitude is rather large as expected from the surface Debye temperature (290 K) determined by RHEPD [12]. Contrarily, electrons penetrate into the bulk where the vibration amplitude is rather suppressed. Therefore, the blurry RHEPD pattern is explained as the effect of thermal diffuse scattering by the topmost atoms [13]. In the case of RHEED pattern, such an effect is suppressed. Indeed, the pattern features are well reproduced by the simulation based on the dynamical diffraction theory as shown in the figure.

3.2 Phase transition of Si(111)-√3×√3-Ag surface In 1989, from the x-ray diffraction study, this surface was proposed to have the honeycomb-chained triangle (HCT) structure [3]. On the other hand, from the scanning tunnelling microscopy (STM) observation and theoretical calculation, the inequivalent triangle (IET) structure is the stable structure at low temperatures [4–6]. This structure has two different phases (IET(+) and IET(-)) where the orderings of the inequivalent triangles are inversed with respect to the [112] axis. The existence of HCT and IET structures are explained as the displacive phase transition among them. Recent photoemission spectroscopy study however suggests that even at room temperature the IET is stable and the phase transition is described as the order-disorder type [7].

Figure 2(a) shows the temperature dependences of the RHEPD spot intensities observed from the Si(111)-√3×√3-Ag surface [14]. The spot intensities increase moderately from room temperature to 120 K. This behaviour is explained by the Debye-Waller factor. The intensities of the (0 0) and (2/3 2/3) spots slightly decrease below 120 K, while that of the (1/3 1/3) spot increases dramatically. These show that the phase transition occurs at a critical temperature T_C = 120 K. The above temperature dependences of the spot intensities are hardly attributed to the displacive phase transition since if assuming it the decreases of the (0 0) and (2/3 2/3) intensities below T_C give a negative Debye temperature which is physically inappropriate. Therefore, we attempted to reproduce the above temperature dependences based on the order-disorder phase transition. Assuming the order-disorder phase transition, at low temperatures a domain is composed of a single phase. At elevated temperatures, the anti-phase component appears in

the domain and eventually two phases coexist in an equal probability. The anti-phase boundaries that separate two different phases of domains disappear. Then, the diffraction intensities are given by

$$I_{hk} = I_{hk}(f) + I_{hk}(1-f) \tag{1}$$

where hk denotes the spot index and f denotes the fraction of IET(+) phase in a IET(+) domain. Figure 2(b) shows the dependences of I_{hk} on f calculated through the dynamical method. According to the phase transition theory, f is given by

$$f = 1/2 + A\left|1 - T/T_C\right|^{\beta} \tag{2}$$

where A is a constant and β is the critical exponent. The solid lines in Fig. 2 are obtained using equations (1) and (2) with the adjustable parameter of β. The experimental features are well reproduced suggesting the validity of the order-disorder phase transition. We found $\beta \sim 0.5$. This indicates that the phase transition can be described in terms of the mean field approximation. Thus, we demonstrate that the Si(111)-√3×√3-Ag undergoes the order-disorder phase transition using the structural analysis.

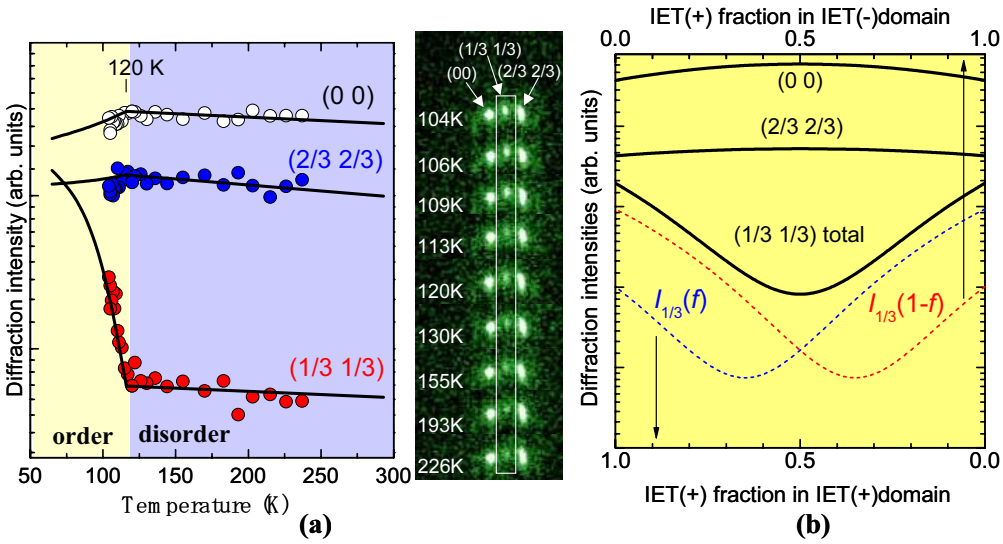

Fig. 2 (a) Temperature dependences of the diffraction spot intensities from the Si(111)-√3×√3-Ag. Solid lines in the figure represent the theoretical diffraction spot intensities using equations (1) and (2). (b) The diffraction spot intensities calculated based on the dynamical diffraction theory using Eq. (1).

3.3 Atomic arrangement of Si(111)-√21×√21-Ag surface This surface is formed by the additional deposition of Ag, Au and alkali metals (0.1-0.2ML) on the Si(111)-√3×√3-Ag surface. The number of possible adsorption sites is 21 in the unit cell. It is believed that three to five Ag atoms are included in the unit cell. Furthermore, there are two choices in the structure of substrate (IET or HCT). Thus, there are a huge number of combinations. So far, the structure of this surface has been studied by STM and x-ray diffraction [8–11]. However, different authors reported different models and a unique model has not yet been determined. We attempted to select the most probable structure using RHEPD.

We attempted to find the best structure, which reproduces both the rocking curves and pattern profiles from the possible combinations. Through the rocking curve analyses, we found that the substrate should be the IET, the number of Ag atoms in the unit cell should be three and all the Ag atoms occupy the large Ag triangle of the IET through the rocking curve analyses. However, there are still five cases that are not discriminated by the rocking curves. Thus, we examined the diffraction patterns. Figure 3 shows the experimental and simulated intensity profiles along the 1/7-th Laue zone. It is seen that the profile of model 3 is clearly distinguished from the others and in good agreement with experiment [15].

In this structure, three Ag atoms sitting on the large Ag triangles surround the Si trimer site and the coupled three Ag atoms are distributed at the corner of the unit cell. The small Ag triangle and Si-trimer are not favoured as the adsorption sites. This agrees with the theoretical prediction. The coupling of three Ag atoms is explained as the cohesive property of Ag atoms. Although the coupled three Ag atoms can surround the Si trimers or small Ag triangles of IET, the former is energetically more favoured. This model also satisfies the three-fold symmetry required from the STM observation.

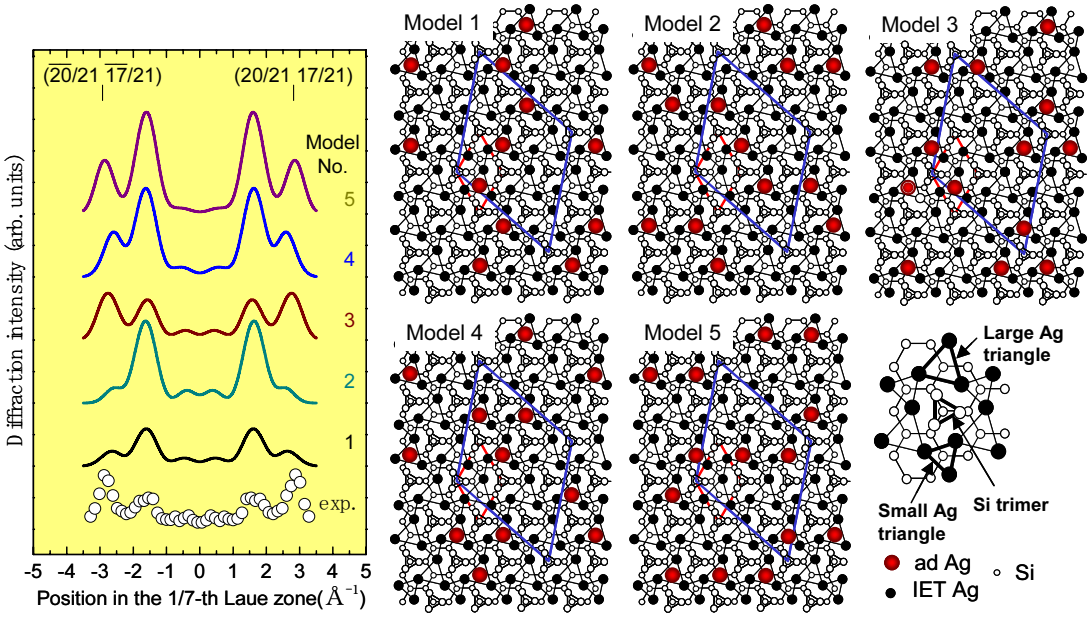

Fig. 3 Intensity profiles along the 1/7-th Laue zone obtained in the experiment and simulations. Simulations were carried out using the models 1 to 5 schematically shown here. Possible adsorption sites in the case of IET structure (Large and small Ag triangles and Si trimer sites) are also shown. Blue and red lines denote the unit cells for the $\sqrt{21}\times\sqrt{21}$ and $\sqrt{3}\times\sqrt{3}$ periodicities

References

[1] A. Ichimiya, Solid State Phenom. **28/29**, 143 (1992/93).
[2] A. Kawasuso, T. Ishimoto, M. Maekawa, Y. Fukaya, K. Hayashi, and A. Ichimiya, Rev. Sci. Instrum. **75**, 4585 (2004).
[3] T. Takahashi, S. Nakatani, N. Okamoto, T. Ishikawa, and S. Kikuta, Jpn. J. Appl. Phys. **27**, L753 (1988).
[4] H. Aizawa, M. Tsukada, N. Sato, and S. Hasegawa, Surf. Sci. **429**, L509 (1999).
[5] H. Tajiri, K. Sumitani, S. Nakatani, A. Nojima, T. Takahashi, K. Akimoto, H. Sugiyama, X. Zhang, and H. Kawata, Phys. Rev. B **68**, 35330 (2003).
[6] N. Sato, T. Nagao, and S. Hasegawa, Surf. Sci. **442**, 65 (1999).
[7] I. Matsuda, H. Morikawa, C. Liu, S. Ohuchi, S. Hasegawa, T. Okuda, T. Kinoshita, C. Ottaviani, A. Cricenti, M. D'angelo, P. Soukiassian, and G. Lay, Phys. Rev. B **68**, 85407 (2003).
[8] J. Nogami, K. J. Wan, and X. F. Lin, Surf. Sci. **306**, 81 (1994).
[9] A. Ichimiya, H. Nomura, Y. Horio, T. Sato, T. Sueyoshi, and M. Iwatsuki, Surf. Rev. Lett. **1**, 1 (1994).
[10] X. Tong, S. Ohuchi, N. Sato, T. Tanikawa, T. Nagao, I. Matsuda, Y. Aoyagi, and S. Hasegawa, Phys. Rev. B **64**, 205316 (2001).
[11] H. Tajiri, K. Sumitani, W. Yashiro, S. Nakatani, T. Takahashi, K. Akimoto, H. Sugiyama, X. Zhang, and H. Kawata, Surf. Sci. **493**, 214 (2001).
[12] Y. Fukaya, A. Kawasuso, and A. Ichimiya, Phys. Rev. B **70**, 245422 (2004).
[13] K. Hayashi, A. Kawasuso, and A. Ichimiya, Surf. Sci. **600**, 4426 (2006).
[14] Y. Fukaya, A. Kawasuso, and A. Ichimiya, e-J. Surf. Sci. Nanotech. **3**, 228 (2005).
[15] Y. Fukaya, A. Kawasuso and A. Ichimiya, Surf. Sci. **600**, 3141 (2006).